



Missouri University of Science and Technology
Scholars' Mine

International Specialty Conference on Cold-Formed Steel Structures

(2014) - 22nd International Specialty Conference on Cold-Formed Steel Structures

Nov 5th, 12:00 AM - 12:00 AM

Developments in the Finite Strip Buckling Analysis of Plates and Channel Sections under Localised Loading

Gregory J. Hancock

Cao Hung Pham

Follow this and additional works at: <https://scholarsmine.mst.edu/isccss>



Part of the [Structural Engineering Commons](#)

Recommended Citation

Hancock, Gregory J. and Pham, Cao Hung, "Developments in the Finite Strip Buckling Analysis of Plates and Channel Sections under Localised Loading" (2014). *International Specialty Conference on Cold-Formed Steel Structures*. 5.

<https://scholarsmine.mst.edu/isccss/22iccfss/session03/5>

This Article - Conference proceedings is brought to you for free and open access by Scholars' Mine. It has been accepted for inclusion in International Specialty Conference on Cold-Formed Steel Structures by an authorized administrator of Scholars' Mine. This work is protected by U. S. Copyright Law. Unauthorized use including reproduction for redistribution requires the permission of the copyright holder. For more information, please contact scholarsmine@mst.edu.

Developments in the Finite Strip Buckling Analysis of Plates and Channel Sections under Localised Loading

Gregory J Hancock¹ and Cao Hung Pham²

Abstract

Thin-walled sections under localised loading may lead to web crippling of the sections. This paper develops the Semi-Analytical Finite Strip Method (SAFSM) for thin-walled sections subject to localised loading to investigate web crippling phenomena. The method is benchmarked against analytical solutions, Finite Element Method (FEM) solutions, as well as Spline Finite Strip Method (SFSM) solutions.

Introduction

Thin-walled sections and plates under localised loading leading to plate buckling have been studied analytically for a long period mainly as part of investigations of web plates of sections at points of concentrated load. Two of the most comprehensive summaries of the work to date have been by Khan and Walker (1972) where the buckling of plates subject to localised loading was investigated and Johansson and Lagerqvist (1995) where the resistance of plate edges to localised loading is summarised. More recently, Natario, Silvestre and Camotim (2012) have further developed these investigations for beams subjected to concentrated loads using Generalised Beam Theory (GBT). They benchmark GBT for plates, un-lipped channels and I-sections against the earlier research and the Shell Finite Element method (SFE). To date, the Finite Strip Method (FSM) of analysis developed by YK Cheung (1976) does not appear to have been used for buckling studies under localised loading. As the Finite Strip Method (FSM) is used extensively in the Direct Strength Method (DSM) of design of cold-formed sections in the North American Specification NAS S100 (AISI, 2102) and the Australian/New Zealand Standard AS/NZS 4600 (Standards Australia, 2005), it is important that the FSM of buckling analysis is extended to localised loading.

¹ Emeritus Professor and Professorial Research Fellow, School of Civil Engineering, The Univ. of Sydney, Sydney NSW 2006, Australia.

² ARC Australian Postdoctoral Fellow, School of Civil Engineering, The Univ. of Sydney, Sydney NSW 2006, Australia.

This paper further develops the Semi-Analytical Finite Strip Method (SAFSM) for thin-walled sections subject to localised loading and benchmarks it against the Spline Finite Strip Method (SFSM) used previously by Pham and Hancock (2009) for shear buckling problems and the Finite Element Method program ABAQUS (Hibbitt, Karsson and Sorenson, 1997).

Folded plate and finite strip theories for the buckling analysis of thin-walled sections and stiffened panels in longitudinal and transverse compression and shear have been developed since the mid-1960s. The solutions of Plank and Wittrick (1974) were based on the SAFSM of analysis developed by YK Cheung (1976). Recently, Chu et al (2005) and Bui (2009) have applied the SAFSM to the buckling of thin-walled sections under more general loading conditions so that multiple series terms are used to capture the modulation of the buckles that occurs. These latter papers are restricted to bending of the sections and transverse compression and shear are not included. The application of the SAFSM to uniform shear of thin-walled sections has recently been applied by Hancock and Pham (2013) where multiple series terms in the longitudinal direction are used to perform the buckling analyses. In the present paper, the method in Hancock and Pham (2013) is extended to include the potential energy resulting from varying longitudinal, transverse and shear stresses. Multiple series terms in the longitudinal direction are used to compute the pre-buckling stresses in the plates and sections, and to perform the buckling analyses using these stresses. Solution convergence with increasing numbers of series terms is provided. The more localised the loading and hence buckling mode, the more series terms are required for accurate solutions especially for longer sections with concentrated loads.

Finite Strip Pre-Buckling and Buckling Analyses

The SAFSM allows the deformations and stresses to be computed for any folded plate system satisfying the boundary conditions assumed. Normally, the sections are assumed simply supported at the ends so that the harmonic functions in the longitudinal direction are orthogonal thus allowing the different series terms to be uncoupled in the linear stiffness analysis. Longitudinal functions for other boundary conditions can be chosen which are also orthogonal as given by Cheung (1976). The resulting stiffness equations are summarised by:

$$[K]\{\delta\} = \{W\} \quad (1)$$

where $[K]$ is the system stiffness matrix based on a strip subdivision of a thin-walled section as shown in Fig. 1, $\{\delta\}$ are the nodal line displacements of the strips in the global X,Y,Z axes, and $\{W\}$ are the nodal line forces (line loads) as also shown in Fig. 1. Equation 1 can be solved for the nodal line displacements

$\{\delta\}$ in the global X,Y,Z axes, and the pre-buckling membrane stresses $\{\sigma\}$ in the strips which are also described by harmonic functions.

Based on the pre-buckling membrane stresses $\{\sigma\}$, the stability equations given by Equation 2 can be derived from the minimum total potential of the system undergoing buckling deformations. Since the buckling deformations also satisfy the simply supported boundary conditions, the same displacement functions are used for the buckling deformations as for the pre-buckling deformations.

$$([K] - \lambda[G])\{\delta\} = 0 \quad (2)$$

where $[G]$ is the system stability matrix and λ is the load factor against buckling.

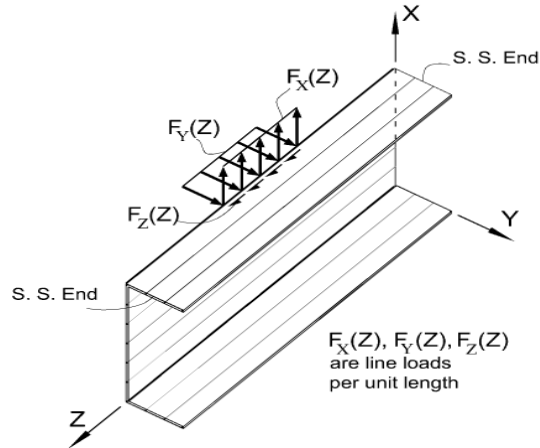


Figure 1. Line loads on channel section showing global axes X,Y,Z

Plate deformations

The plate flexural deformations w of a strip can be described by the summation over μ series terms as:

$$w = \sum_{m=1}^{\mu} f_{1m}(y) \cdot X_{1m}(x) \quad (3)$$

where w is in the z-direction perpendicular to the strip as shown in Fig. 2.

The function $f_{1m}(y)$ for the m th series term is the transverse variation given by:

$$f_{1m}(y) = \alpha_{1Fm} + \alpha_{2Fm} \cdot \left(\frac{y}{b}\right) + \alpha_{3Fm} \cdot \left(\frac{y}{b}\right)^2 + \alpha_{4Fm} \cdot \left(\frac{y}{b}\right)^3 \quad (4)$$

where the 4 polynomial coefficients α_{iFm} for the m th series term depend on the nodal line deformations of the strip. The term b is the width of the strip.

The function $X_{1m}(x)$ is the longitudinal variation of the m th series term and is given by:

$$X_{1m}(x) = \sin\left(\frac{m\pi x}{L}\right) \quad (5)$$

where L is the length of the strip. The function $X_{1m}(x)$ satisfies the simply supported boundary conditions assumed in this paper. Other boundary conditions can be used in the SAFSM as set out in Cheung (1976) but are not considered in this paper.

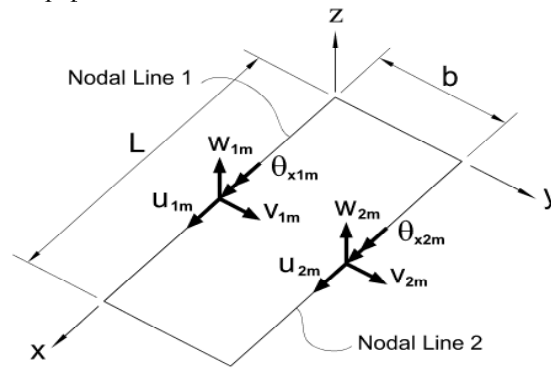


Fig. 2. Strip local axes x, y, z and nodal line deformations for the m th series term

The plate membrane deformations (u, v) in the (x, y) directions respectively can be described by the summation over μ series terms as:

$$v = \sum_{m=1}^{\mu} f_{vm}(y) \cdot X_{1m}(x) \quad (6)$$

$$u = \sum_{m=1}^{\mu} f_{um}(y) \cdot X'_{1m}(x) \cdot \frac{L}{m\pi} \quad (7)$$

The functions $f_{um}(y)$ and $f_{vm}(y)$ are the transverse variations given by:

$$f_{vm}(y) = \alpha_{1Mm} + \alpha_{2Mm} \cdot \left(\frac{y}{b}\right) \quad (8)$$

$$f_{um}(y) = \alpha_{3Mm} + \alpha_{4Mm} \cdot \left(\frac{y}{b}\right) \quad (9)$$

where the 4 polynomial coefficients α_{iMm} for the m th series term depend on the nodal line deformations of the strip.

The nodal line flexural deformations $\{\delta_{Fm}\} = (w_{1m}, \theta_{x1m}, w_{2m}, \theta_{x2m})^T$ in Fig. 2 can be related to the polynomial coefficients in (4) above by:

$$\{\delta_{Fm}\} = [C_F]\{\alpha_{Fm}\} \quad (10)$$

where $\{\alpha_{Fm}\} = (\alpha_{1Fm} \quad \alpha_{2Fm} \quad \alpha_{3Fm} \quad \alpha_{4Fm})^T$

Similarly, the nodal line membrane deformations $\{\delta_{Mm}\} = (u_{1m}, v_{1m}, u_{2m}, v_{2m})^T$ in Fig. 2 can be related to the polynomial coefficients in (8) and (9) above by:

$$\{\delta_{Mm}\} = [C_M]\{\alpha_{Mm}\} \quad (11)$$

where $\{\alpha_{Mm}\} = (\alpha_{1Mm} \quad \alpha_{2Mm} \quad \alpha_{3Mm} \quad \alpha_{4Mm})^T$

The matrices $[C_F]$ and $[C_M]$ have inverses $[C_F]^{-1}$, $[C_M]^{-1}$ which are given in Hancock and Pham (2014). The resulting equations for the plate flexural and membrane deformations are given by:

$$w = \sum_{m=1}^{\mu} X_{1m} [\Gamma_{FL}] [C_F]^{-1} \{\delta_{Fm}\} \quad (12)$$

where $[\Gamma_{FL}] = [1 \quad (y/b) \quad (y/b)^2 \quad (y/b)^3]$ (13)

$$u = \sum_{m=1}^{\mu} X'_{1m} \cdot \frac{L}{m\pi} [\Gamma_{Mu}] [C_M]^{-1} \{\delta_{Mm}\} \quad (14)$$

where $[\Gamma_{Mu}] = [0 \quad 0 \quad 1 \quad (y/b)]$ (15)

$$v = \sum_{m=1}^{\mu} X_{1m} [\Gamma_{Mv}] [C_M]^{-1} \{\delta_{Mm}\} \quad (16)$$

where $[\Gamma_{Mv}] = [1 \quad (y/b) \quad 0 \quad 0]$ (17)

In the computation of the potential energy described later, derivatives of the plate flexural and membrane deformations are required. The derivatives used are as follows:

$$\frac{\partial w}{\partial x} = \sum_{m=1}^{\mu} [\Gamma_{FL}] X'_{1m} \{\alpha_{Fm}\} \quad (18)$$

$$\frac{\partial w}{\partial y} = \sum_{m=1}^{\mu} \frac{1}{b} [\Gamma_{FT}] X_{1m} \{\alpha_{Fm}\} \quad (19)$$

where $[\Gamma_{FT}] = [0 \quad 1 \quad 2(y/b) \quad 3(y/b)^2]$ (20)

$$\frac{\partial u}{\partial x} = \sum_{m=1}^{\mu} X'_{1m} \cdot \frac{L}{m\pi} [\Gamma_{Mu}] \{\alpha_{Mm}\} \quad (21)$$

$$\frac{\partial v}{\partial x} = \sum_{m=1}^{\mu} X'_{1m} [\Gamma_{Mv}] \{\alpha_{Mm}\} \quad (22)$$

Membrane stresses

The plate membrane theory is that used by Cheung (1976) and is given by:

$$\{\sigma\} = [D_M]\{\varepsilon\} \quad (23)$$

$$[D_M] = \begin{bmatrix} E_1 & \nu E_1 & 0 \\ \nu E_1 & E_1 & 0 \\ 0 & 0 & G \end{bmatrix} \quad (24)$$

$$\{\sigma\} = (\sigma_x \quad \sigma_y \quad \tau_{xy})^T \quad (25)$$

$$\{\varepsilon\} = \left[\frac{\partial u}{\partial x} \quad \frac{\partial v}{\partial y} \quad \frac{\partial u}{\partial y} + \frac{\partial v}{\partial x} \right]^T \quad (26)$$

with the plate membrane rigidity $E_1 = E/(1-\nu^2)$, and where G is the shear modulus $= E/2(1+\nu)$. Substitution for v from (16) and u from (14) in (26) allows the membrane stresses to be computed from the nodal line deformations using (23). Note that the normal stresses vary as the sine function whereas the shear stresses vary as the cosine function.

Strain energy and potential energy

In order to compute the stiffness and stability matrices of the strip according to conventional finite strip theory (Cheung, 1976), it is necessary to define the strain energy in the strip under deformation and the potential energy of the membrane forces.

The flexural strain energy U_F is given by:

$$U_F = \frac{1}{2} \int_0^L \int_0^b \left(-M_x \frac{\partial^2 w}{\partial x^2} - M_y \frac{\partial^2 w}{\partial y^2} + 2M_{xy} \frac{\partial^2 w}{\partial x \partial y} \right) dy dx \quad (27)$$

The membrane strain energy U_M is given by:

$$U_M = \frac{1}{2} \int_0^L \int_0^b (\sigma_x \varepsilon_x + \sigma_y \varepsilon_y + \tau_{xy} \gamma_{xy}) dy dx \quad (28)$$

The flexural potential energy of the membrane forces V_F is given by:

$$V_F = -\frac{1}{2} \int_0^L \int_0^b \left(\sigma_x(x) \cdot \left(\frac{\partial w}{\partial x} \right)^2 + \sigma_y(x) \cdot \left(\frac{\partial w}{\partial y} \right)^2 + 2\tau_{xy}(x) \left(\frac{\partial w}{\partial x} \right) \left(\frac{\partial w}{\partial y} \right) \right) t dy dx \quad (29)$$

where $\sigma_x(x)$, $\sigma_y(x)$, and $\tau_{xy}(x)$ are the assumed membrane normal and shear stresses with the signs given in Fig. 3, and t is the plate thickness.

The transverse stress and shear stress in a strip are each assumed uniform across the strip width and computed from the means on the two nodal lines. The resulting membrane stresses can be described by harmonic functions in the longitudinal direction and linear or constant functions in the transverse direction as follows:

$$\begin{aligned} \sigma_x(x) &= \left(\sigma_1(x) + (\sigma_2(x) - \sigma_1(x)) \cdot \left(\frac{y}{b} \right) \right) \\ &= \sum_{k=1}^{\mu} \sigma_k(x) \cdot (\sigma_{1k} + (\sigma_{2k} - \sigma_{1k}) \cdot \left(\frac{y}{b} \right)) \end{aligned} \quad (30)$$

where
$$\sigma_k(x) = \sin\left(\frac{k\pi x}{L}\right) \tag{31}$$

$$\sigma_y(x) = \sum_{k=1}^{\mu} \sigma_k(x) \cdot (\sigma_{Tk}) \tag{32}$$

$$\tau_{xy}(x) = \sum_{k=1}^{\mu} \tau_k(x) \cdot (\tau_k) \tag{33}$$

where
$$\tau_k(x) = \cos\left(\frac{k\pi x}{L}\right) \tag{34}$$

Substitution of Equations 30, 32 and 33 in Equation 29 using Equations 18 and 19 results in

$$V_F = V_{FL} + V_{FT} + V_{FS1} + V_{FS2} \tag{35}$$

where

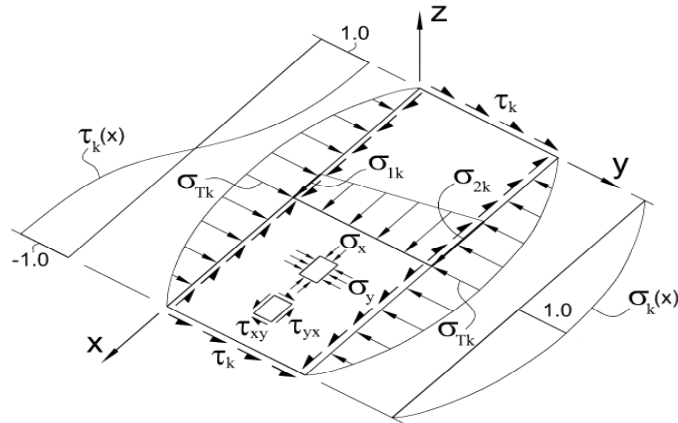


Figure 3. Assumed membrane stresses (k = 1)

$$V_{FL} = -\frac{1}{2} \int_0^L \int_0^b \sum_{m=1}^{\mu} \sum_{n=1}^{\mu} \{\alpha_{Fm}\}^T [\Gamma_{FL}]^T X'_{1m} \cdot \sum_{k=1}^{\mu} \sigma_k(x) \cdot (\sigma_{1k} + (\sigma_{2k} - \sigma_{1k}) \cdot \left(\frac{y}{b}\right)) [\Gamma_{FL}] X'_{1n} \{\alpha_{Fn}\} t dx dy \tag{36}$$

$$V_{FT} = -\frac{1}{2} \int_0^L \int_0^b \sum_{m=1}^{\mu} \sum_{n=1}^{\mu} \{\alpha_{Fm}\}^T [\Gamma_{FT}]^T \frac{1}{b} X_{1m} \cdot \sum_{k=1}^{\mu} \sigma_k(x) \cdot (\sigma_{Tk}) [\Gamma_{FT}] \frac{1}{b} X_{1n} \{\alpha_{Fn}\} t dy dx \tag{37}$$

$$V_{FS1} = -\frac{1}{2} \int_0^L \int_0^b \sum_{m=1}^{\mu} \sum_{n=1}^{\mu} \{\alpha_{Fm}\}^T [\Gamma_{FL}]^T X'_{1m} \cdot \sum_{k=1}^{\mu} \tau_k(x) \cdot (\tau_k) [\Gamma_{FT}] \frac{1}{b} X_{1n} \{\alpha_{Fn}\} t dy dx \tag{38}$$

$$V_{FS2} = -\frac{1}{2} \int_0^L \int_0^b \sum_{m=1}^{\mu} \sum_{n=1}^{\mu} \{\alpha_{Fm}\}^T [\Gamma_{FT}]^T \frac{1}{b} X_{1m} \cdot \sum_{k=1}^{\mu} \tau_k(x) \cdot (\tau_k) [\Gamma_{FL}] X'_{1n} \{\alpha_{Fn}\} t dy dx \quad (39)$$

The membrane potential energy of the membrane forces V_M is given by:

$$V_M = -\frac{1}{2} \int_0^L \int_0^b (\sigma_x(x) \left(\frac{\partial u}{\partial x}\right)^2 + \sigma_x(x) \left(\frac{\partial v}{\partial x}\right)^2) t dy dx \quad (40)$$

Substitution of Equation 30 in Equation 40 using Equations 21 and 22 results in

$$V_M = V_{Mu} + V_{Mv} \quad (41)$$

where

$$V_{Mu} = -\frac{1}{2} \int_0^L \int_0^b \sum_{m=1}^{\mu} \sum_{n=1}^{\mu} \{\alpha_{Mm}\}^T [\Gamma_{Mu}]^T X'_{1m} \frac{L}{m\pi} \cdot \sum_{k=1}^{\mu} \sigma_k(x) \cdot (\sigma_{1k} + (\sigma_{2k} - \sigma_{1k}) \cdot \left(\frac{y}{b}\right)) [\Gamma_{Mu}] X'_{1n} \frac{L}{n\pi} \{\alpha_{Mn}\} t dy dx \quad (42)$$

$$V_{Mv} = -\frac{1}{2} \int_0^L \int_0^b \sum_{m=1}^{\mu} \sum_{n=1}^{\mu} \{\alpha_{Mm}\}^T [\Gamma_{Mv}]^T X'_{1m} \cdot \sum_{k=1}^{\mu} \sigma_k(x) \cdot (\sigma_{1k} + (\sigma_{2k} - \sigma_{1k}) \cdot \left(\frac{y}{b}\right)) [\Gamma_{Mv}] X'_{1n} \{\alpha_{Mn}\} t dy dx \quad (43)$$

Stiffness and stability matrices

For equilibrium, the theorem of minimum total potential energy of the flexural energy with respect to each of the elements $\{\delta_{Fm}\}$ is:

$$\frac{\partial(U_F+V_F)}{\partial\{\delta_{Fm}\}} = 0 \quad (44)$$

The result is:

$$[k_{Fm}]\{\delta_{Fm}\} + \sum_{n=1}^{\mu} [g_{Fmn}]\{\delta_{Fn}\} = 0 \quad m = 1, 2, \dots, \mu \quad (45)$$

The matrices $[k_{Fm}]$ and $[g_{Fmn}]$ are given in Hancock and Pham (2014). The integrals can be evaluated exactly for the harmonic functions satisfying the simply supported boundary conditions.

For equilibrium, the theorem of minimum total potential for the membrane energy is:

$$\frac{\partial(U_M+V_M)}{\partial\{\delta_{Mm}\}} = 0 \quad (46)$$

The result is:

$$[k_{Mm}]\{\delta_{Mm}\} + \sum_{n=1}^{\mu} [g_{Mmn}]\{\delta_{Mn}\} = 0 \quad m = 1, 2, \dots, \mu \quad (47)$$

The matrices $[k_{Mm}]$ and $[g_{Mmn}]$ are given in Hancock and Pham (2014). The integrals have been evaluated exactly for the harmonic functions satisfying the simply supported boundary conditions.

For folded plate assemblies including thin-walled sections such as channels, (45) and (47) must be transformed to a global co-ordinate system to assemble the stiffness $[K_m]$ and stability $[G_{mn}]$ matrices of the folded plate assembly or section.

A computer program **bfinst10.cpp** has been written in Visual Studio C++ to assemble the stiffness equations and stability equations to solve for the pre-buckling displacements and pre-buckling stresses using equations 1 and 23, then buckling load factors (eigenvalues) and buckling modes (eigenvectors) using Equations 2, 45 and 47. The matrix $[G]$ has $4 * N * \mu$ degrees of freedom where N is the number of nodal lines and μ is the number of series terms. If the rows and columns in the matrix $[G]$ are organised so that each degree of freedom is taken over the μ series terms, then the half-bandwidth of the matrix is simply μ times the half-bandwidth of the problem with one series term. This speeds the computation of the eigenvalues and eigenvectors considerably.

Solutions for plate simply supported on all four edges with localised loading at centre

The solutions for a plate of length L simply supported along all four edges determined using the **bfinst10.cpp** analysis is compared with the solution based on the equation of Johansson and Lagerqvist (1995), the Spline Finite Strip Method (SFSM) (Pham and Hancock 2009) and the Finite Element Method program ABAQUS (Hibbitt, Karsson and Sorenson 1997). The equation for the elastic buckling of a rectangular plate is given as:

$$\sigma_{cr} = \frac{k \pi^2 E}{12(1-\nu^2) (h/t)^2} / \left(\frac{n}{h}\right) \quad (48)$$

where n is the length of the loaded portion subject to the stress σ_{cr} , h is the depth of the plate which may consist of multiple strips and k is the plate buckling coefficient for transverse compression.

The analysis is carried out for 8 equal width strips and an increasing number of series terms. Load length ratios (n/L) of 0.025, 0.05, 0.200 and 0.250 and aspect ratios (h/L) of 1:1, 1:5 and 1:10 have been investigated and the solutions for the buckling coefficient k are compared in Table 1 with those of Johansson and

Lagerqvist (1995), the SFSM where 8 strips and 80 splines have been used, and the FEM where 5mm square elements have been used.

Load length ratio (n/L)	Aspect ratio (L/h)	Johansson and Lagerqvist (1995)	SFSM	FEM (ABAQUS)	SAFSM (bfinst10.cpp) (series terms in brackets)
0.250	1.0	3.450	3.383	3.399	3.480 (5) 3.478 (11)
0.050	2.0	2.409	2.360	2.368	2.421(5) 2.404(11) 2.404(15)
0.200	2.0	2.544	2.508	2.515	2.549 (5) 2.545 (11)
0.050	5.0	2.178	1.983	1.991	2.066 (11) 2.018 (19)
0.200	5.0	2.628	2.582	2.590	2.697 (7) 2.597 (11)
0.025	10.0	2.138	1.392	1.392	1.433 (25)

Table 1. Buckling coefficients k for simply supported rectangular plates under localised load along one longitudinal edge at the centre of the plate

It is clear that the SAFSM solutions become more accurate with increasing numbers of series terms, and that more terms are required for higher aspect ratios and lower load length ratios. The solutions converge to values slightly higher than those of the SFSM and FEM. Five series terms seem adequate for square plates and plates with an aspect ratio of 2.0. However, for higher aspect ratios such as $L/h = 5.0$, at least 11 series terms are necessary and 19 series terms are needed to achieve accuracies better than 2% when the load length ratio $n/L = 0.05$. This is a fairly concentrated load on a longer length. For an aspect ratio of 10, an accuracy better than 3% is achieved with 25 series terms. It is interesting to note that the equation of Johansson and Lagerqvist (1995) is not accurate for aspect ratios of 5.0 and 10.0.

The buckling mode for an aspect ratio (L/h) of 5:1, a load length ratio (n/L) of 0.20 and 11 series terms determined from bfinst10.cpp is plotted in Fig. 4.

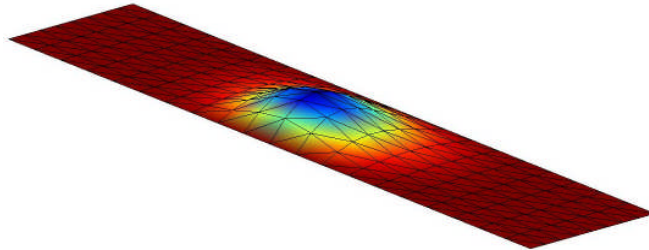


Figure 4. Rectangular plate buckling mode single edge loading
 $L/h = 5.0$, $n/h = 1.0$

Lipped channel section under localised loading

A 200 mm deep lipped channel with flange width 80mm, lip length 20 mm as studied by Pham and Hancock (2009) and Hancock and Pham (2013) has been investigated. These dimensions are all centreline and not overall. In Pham and Hancock (2009), the section studied was 2 mm thick. This has been reduced to 1 mm to match with the 200 mm deep plate simply supported on all four edges in the previous section. Further, the section now contains rounded corners with an internal radius of 5 mm. The strip subdivision used is 1, 4, 8, 4 strips for each of the lips, flanges, the web and each of the corners respectively making 34 strips in total with 35 nodal lines. The length is 1000 mm and the loading applied is along a length $n = 200$ mm or $n = 50$ mm at the centre and located at the junction of the corner and top flange for IOF loading and also at the junction of the corner and bottom flange for ITF loading. These nodal lines are also assumed to be prevented against lateral deflection in the direction perpendicular to the web and load. Two different sets of boundary conditions have been used in the FEM analysis for comparison. These are the web only simply supported (SS), and the web, flange and lip simply supported (i.e. no buckling deformation in the plane of the cross section at the ends but free to deform longitudinally). The latter boundary conditions are the same as assumed in the SAFSM analysis with the simply supported harmonic functions.

The buckling loads are given in kN in Table 2. The SAFSM solutions are close to the FEM web, flange and lip simply supported cases as would be expected since these are the boundary conditions assumed for the simply supported boundary conditions of all strips. The buckling coefficients according to Eq. 48 are also given in Table 2 and can be compared with those in Table 1. The buckling coefficients are more than 2.5 times those for the simple plate in Table 1. The SAFSM (bfinst10.cpp) solutions with 7 series terms are accurate to better than 0.2% when compared with the FEM solutions for both the IOF and ITF loading cases when $n/L = 0.20$ (200mm case). They are accurate to better than 1.0% with 15 series terms when $n/L = 0.05$ (50mm case).

Loading Case	Length (mm)	FEM (ABAQUS)	FEM (ABAQUS)	SAFSM (bfinst10)	Buckling Coefficient in Eq. 48
	Load length (mm)	Web only SS	Web, flange and lip SS	(series terms in brackets)	k
IOF	1000	5.410	6.009	6.024 (7)	6.665 (7)
	200			6.017 (11)	6.657 (11)
				6.016 (15)	6.656 (15)
ITF	1000	2.731	3.056	3.051 (7)	3.375 (7)
	200			3.049 (11)	3.374 (11)
				3.049 (15)	3.374 (15)
IOF	1000	4.766	5.175	5.303 (7)	5.867 (7)
	50			5.234 (11)	5.791 (11)
				5.221 (15)	5.778 (15)
ITF	1000	2.472	2.727	2.746 (7)	3.039 (7)
	50			2.737 (11)	3.028 (11)
				2.735 (15)	3.026 (15)

Table 2 Lipped channel buckling loads in kN and coefficients k

The buckling mode for the IOF case with $L = 1000$ mm and $n = 200$ mm is shown in Fig. 7.

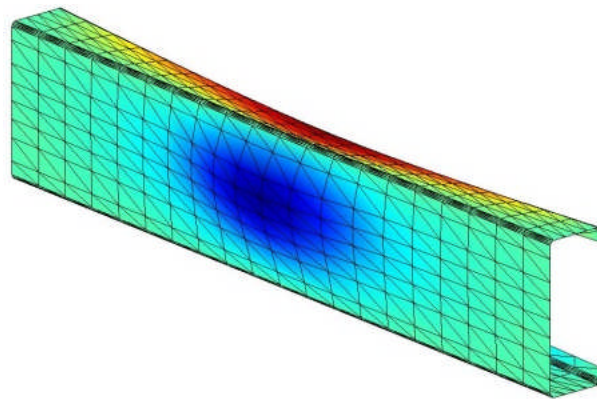


Figure 7. Lipped channel with IOF central load at flange/corner junction
 $n = 200$ mm, $L = 1000$ mm

Web-stiffened channel under localised loading

A 200 mm deep lipped channel with flange width 80 mm, lip length 20 mm, web stiffener with a rectangular indent of 5 mm over a depth of 80 mm located symmetrically about the centre of the web, as studied by Pham and Hancock (2009) and Hancock and Pham (2013) has been investigated. These dimensions are all centreline and not overall. In Hancock and Pham (2013), the section studied was 2 mm thick. This has been reduced to 1 mm to match with the 200 mm deep plate simply supported on all four edges in the previous section. The section now contains rounded corners with an internal radius of 5 mm. The strip subdivision used is 1, 4, 4, 1, 4 strips for each of the lips, flanges, the web flats, web stiffeners and each of the corners respectively making 40 strips in total with 41 nodal lines. The SAFSM (bfinst10.cpp) solutions shown in Table 3 with 25 series terms produce an accuracy better than 2.0% when compared with the FEM solutions for the IOF loading case when $n/L = 0.05$ (50 mm case) and the flange, web and lip are simply supported. Localisation of the buckle in the flange as shown in Fig. 8 requires more series terms than for the simple lipped channel shown in Fig. 7 where localization does not occur. The buckling coefficients k for the IOF case are more than four times those for the simply supported plate in Table 1.

Loading Case	Length (mm)	FEM (ABAQUS)	FEM (ABAQUS)	SAFSM (bfinst10.cpp)	Buckling Coefficient in Eq. 48
	Loading Length (mm)	Web only SS	Web, flange and lip SS	(series terms in brackets)	k
IOF	1000 50	6.725	7.894	8.526 (7)	9.432 (7)
				8.421 (15)	9.317 (15)
				8.212 (21)	9.085 (21)
				8.063 (25)	8.921 (25)
ITF	1000 50	4.152	5.417	5.482 (7)	6.066 (7)
				5.480 (11)	6.062 (11)
				5.475 (15)	6.058 (15)

Table 3 Web-stiffened channel buckling loads in kN and coefficients k

The loads for the case of web only simply supported computed using the FEM are considerably lower than the flange, web and lip simply supported case and demonstrate that this problem is more sensitive to the end boundary conditions

than the simple lipped channel. Alternative orthogonal functions $X_{1m}(x)$ according to Cheung (1976) are under investigation for this case and other boundary conditions such as the end one flange EOF and end two flange ETF loading cases.

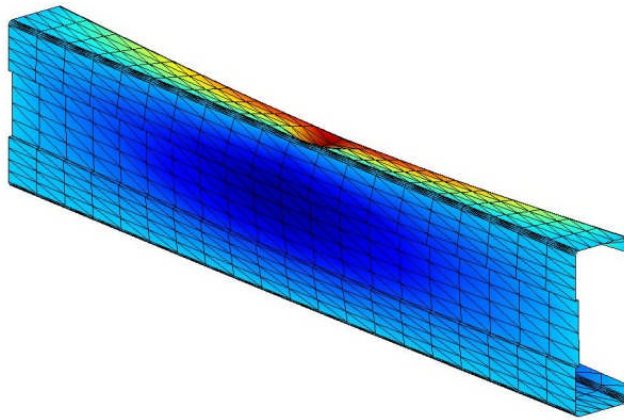


Figure 8 Web-stiffened channel with IOF central load $n = 50\text{mm}$ $L = 1000\text{mm}$

Conclusions

A semi-analytical finite strip method (SAFSM) buckling analysis of thin-walled section subjected to localised loading has been developed and benchmarked against spline finite strip method (SFSM) and finite element method (FEM) solutions. The method has proven to be accurate and efficient compared with the SFSM and FEM methods. The more localised the load, and the longer the section under load then the greater the number of series terms required.

Acknowledgement

Funding provided by the Australian Research Council Discovery Project Grant DP110103948 has been used to perform this project. The SFSM program used was developed by Gabriele Eccher and the graphics program was developed by Song Hong Pham.

References

- American Iron and Steel Institute (AISI) (2007), "North American Specification for the Design of Cold-Formed Steel Structural Members." 2007 Edition, AISI S100-2007.
- Bui, H.C. (2009), "Buckling Analysis of Thin-Walled Sections under General Loading Conditions", *Thin-Walled Structures*, Vol. 47, pp 730-739.
- Cheung, Y.K. (1976), *Finite Strip Method in Structural Analysis*, Pergamon Press, Inc. New York, N.Y.
- Chu, X.T, Ye, Z.M., Kettle, R., Li, L.Y. (2005), "Buckling Behaviour of Cold-Formed Channel Sections under Uniformly Distributed Loads", *Thin-Walled Structures*, Vol. 43, pp 531-542.
- Hancock, G.J. and Pham, C.H. (2013), "Shear Buckling of Channel Sections with Simply Supported Ends using the Semi-Analytical Finite Strip Method", *Thin-Walled Structures*, Vol. 71, pp 72-80.
- Hancock, G.J. and Pham, C.H. (2014), "Buckling Analysis of Thin-Walled Sections under Localised Loading using the Semi-Analytical Finite Strip Method", *International Conference on Thin-Walled Structures*, Busan, Korea,
- Hibbitt, Karsson and Sorenson, Inc. (HKS) (1997) *ABAQUS/standard user's manual*, version 5.7; 1997.
- Johansson, B.J. and Lagerqvist, O. (1995), "Resistance of Plate Edges to Concentrated Forces", *Journal of Constructional Steel Research*, Vol 32, pp 69-105.
- Khan, M.Z. and Walker, A.C. (1972), "Buckling of Plates subjected to Localised Edge Loading", *The Structural Engineer*, Vol 50, No. 6 (June), pp 225-232.
- Nataro, P, Silvestre, N. and Camotim, D. (2012), "Localized Web Buckling Analysis of Beams subjected to Concentrated Loads using GBT", *Thin-Walled Structures*, Vol. 61, pp 27-41.
- Pham, C. H., and Hancock, G. J. (2009). "Shear Buckling of Thin-Walled Channel Sections." *Journal of Constructional Steel Research*, Vol. 65, No. 3, pp. 578-585.
- Plank, R. J., and Wittrick, W. H. (1974), "Buckling Under Combined Loading of Thin, Flat-Walled Structures by a Complex Finite Strip Method", *International Journal for Numerical Methods in Engineering*, Vol. 8, No. 2, pp 323-329.
- Standards Australia. (2005). "AS/NZS 4600:2005, Cold-Formed Steel Structures." Standards Australia/ Standards New Zealand.